

# MATHEMATICAL MODELS FOR METALLURGICAL SCALE-UP

S. A. Halvorsen<sup>1</sup>, R. Schlanbusch<sup>1</sup> and S. Shinkevich<sup>1</sup>

<sup>1</sup>Teknova AS, Gimlemoen 19, NO-4630 Kristiansand, Norway; sah@teknova.no

## ABSTRACT

*Adequate scale-up know-how is to a large degree missing in the metallurgical industry, and the use of new processes is frequently increased only by a few percent at a time.*

*We have applied mathematical analysis to study various aspects of scale-up. A fundamental approach has been chosen where the appropriate model equations have been developed and analyzed. The basic method is described in detail for thermal scale-up, and then summarized for electrical scale-up. The analysis has revealed which non-dimensional groups are involved, and how they are affected by scale-up or scale-down. This allows us to derive general trends, along with time constants, simplified models, etc.*

*Real cases from the industry have been studied. We considered:*

- *General resistive slag reactors*
- *DC electrodes*
- *Thin casting (of silicon)*
- *Acheson process*
- *Metal droplets in slag (metal/slag separation)*

*General guidelines for studying scale-up are suggested based on our experience.*

*Our studies show that appropriate models are powerful tools to reveal general trends and what needs to be further studied either by numerical simulations, laboratory experiments, and/or pilot studies. We therefore recommend that our methodology is applied for evaluating scale-up issues.*

## 1 INTRODUCTION

Due to lack of adequate scale-up know-how the metallurgical industry has increased the scale by only a few percent at a time for new processes; or even worse, the full-scale facilities assembled that do not work or work with capacities far below their target. Similarly, when an industrial full-scale problem needs to be studied, proper scale-down knowledge (how to select the proper pilot and/or laboratory studies) is frequently missing.

To improve the conditions Teknova has run a project on Metallurgical Scale-up in close cooperation with four major metallurgical companies in Norway and with academic partners from the University of Oxford, UK, University of Santiago the Compostela (USC), Spain, University of Agder (UiA), Norway, and Norwegian University of Science and Technology (NTNU), Norway.

Real cases from the industry have been studied. We choose a fundamental approach where the appropriate model equations have been developed and analyzed. Such analysis reveals which non-dimensional groups are involved, and how they are affected by scale-up or scale-down. This allows us to derive general scale-up guidelines, along with time constants, simplified models, etc., supported by results obtained from numerical simulations.

In this paper, we will present the general method in some detail for thermal scale-up and give some results for electrical scale-up before presenting results from some case studies.

## 2 EQUATION ANALYSIS FOR SCALE-UP

### 2.1 Thermal Scale-up

We start by a simple case and consider heat balance within a simple cuboid as shown in Figure 1. Let the L-edge be parallel to the x-axis, the W-edge to the y-axis and H to the z-axis.<sup>2</sup> Then the heat balance equation can be written as:

$$\rho c_p \frac{\partial T}{\partial t} = \frac{\partial}{\partial x} \left( k \frac{\partial T}{\partial x} \right) + \frac{\partial}{\partial y} \left( k \frac{\partial T}{\partial y} \right) + \frac{\partial}{\partial z} \left( k \frac{\partial T}{\partial z} \right) + Q \quad (1)$$

where  $T$  is the temperature;

$\rho$  is the density,  $c_p$  the heat capacity and  $k$  the heat conductivity;

$Q$  is a heat source, due to electric heating and/or chemical reactions;

<sup>2</sup> Please observe that the “thin direction” in Figure 1 is parallel to the x-axis. Hence, the thin plate approximation, equations (4) and (5), describe a vertical plate.

The boundary conditions are given by

$$q = -k \frac{\partial T}{\partial n} = h(T - T_a) \quad (2)$$

where  $q$  is the normal outward heat flux at a boundary;

$\frac{\partial T}{\partial n}$  is the partial derivative of  $T$  in the direction of the outward normal vector;

$h$  is a heat transfer coefficient and  $T_a$  the ambient temperature;

The heat transfer coefficient,  $h$ , can be a function of the temperature, which implies that the boundary condition, (2), is very general. A pure radiation condition can, for instance, be written as:

$$q = \varepsilon \sigma (T^4 - T_a^4) = \varepsilon \sigma (T^2 + T_a^2)(T + T_a)(T - T_a), \quad h = \varepsilon \sigma (T^2 + T_a^2)(T + T_a) \quad (3)$$

where  $\varepsilon$  is the effective emissivity;

$\sigma$  is the Stefan–Boltzmann constant;

We then introduce some non-dimensional tilde-variables defined by  $x = L\tilde{x}$ ,  $y = W\tilde{y}$ ,  $z = H\tilde{z}$ ,  $t = \tau\tilde{t}$  and  $T = T_0 + (T_m - T_0)\tilde{T}$ ; where  $T_0$  is a reference temperature (normally equal to  $T_a$ ),  $T_m$  is the maximum temperature and  $\tau$  a time constant (to be defined). To simplify the following discussion, constant parameters are assumed.

Inserting the tilde definitions in equation (1), we get, after some rearrangement:

$$\left( \frac{L^2 \rho c_p}{k \tau} \right) \frac{\partial \tilde{T}}{\partial \tilde{t}} = \frac{\partial^2 \tilde{T}}{\partial \tilde{x}^2} + \frac{L^2}{W^2} \frac{\partial^2 \tilde{T}}{\partial \tilde{y}^2} + \frac{L^2}{H^2} \frac{\partial^2 \tilde{T}}{\partial \tilde{z}^2} + \frac{L^2}{k(T_m - T_0)} Q$$

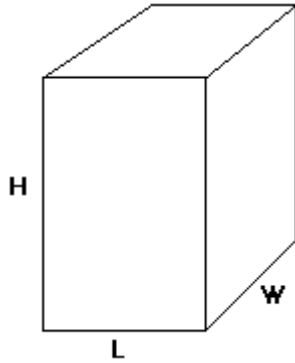


Figure 1: A simple cuboid

From equation (4) we immediately see that if  $W$  is slightly more than 3 times  $L$ , then the coefficient in front of the second term on the right hand side is less than 0.1, and this term can be dropped as a first approximation. Similarly, if  $H$  is slightly more than 3 times  $L$ , then also the third term can be disregarded. Hence, the thin plate approximation is reasonable even at aspect ratios up to 1:3. The heat balance equation then simplifies to:

$$\left( \frac{L^2 \rho c_p}{k \tau} \right) \frac{\partial \tilde{T}}{\partial \tilde{t}} = \frac{\partial^2 \tilde{T}}{\partial \tilde{x}^2} + \frac{L^2}{k(T_m - T_0)} Q \quad (5)$$

with non-dimensional variables, and in standard form as:

$$\rho c_p \frac{\partial T}{\partial t} = \frac{\partial}{\partial x} \left( k \frac{\partial T}{\partial x} \right) + Q \quad (6)$$

Such approximations can only be done after a *proper* scaling, that is the variation of the tilde-variables should be from zero to one (at least approximately).

The structure can be characterized as thermally thin or thick based on the aspect ratios. If at least one aspect ratio ( $L/W$ ,  $L/H$ ,  $W/L$ ,  $W/H$ ,  $H/L$ ,  $H/W$ ) is less than 1/3, the structure is thermally thin with respect to inner heat flow and the equation can be simplified.<sup>3</sup> If not, it should be treated as a thermally thick structure, i.e. 3D heat flow should be applied (unless the problem can be simplified due to some symmetry).

The value of  $\tau$  that makes the coefficient of the left hand side of (4) equal to one defines the time constant:

$$\tau = \frac{L^2 \rho c_p}{k} \quad (7)$$

This is a time constant for obtaining thermal equilibrium due to heat flow in the  $x$ -direction. Similarly, the value of  $Q$  that makes the last term equal to one, defines a characteristic heat density. This is the power density that can maintain a stationary temperature difference of roughly  $(T_m - T_0)$ :<sup>4</sup>

<sup>3</sup> A threshold of 1/3 for aspect ratios is appropriate for a first approximation. Then terms with coefficients less than (approximately) 0.1 are removed from equation (4). A lower threshold should be chosen if more accuracy is required.

<sup>4</sup> The time constant and the characteristic heat density are only rough estimates. A solution of the simplified equation, or further evaluation, is required for more accurate values.

$$Q_0 = \frac{k(T_m - T_0)}{L^2} \quad (8)$$

Observe that there is a *quadratic* dependence on the geometric parameter,  $L$ , in both cases.

The boundary conditions can be non-dimensionalized similarly to the full equation. Assuming that the normal vector is in the x-direction, we get (assuming  $T_a = T_0$ ):

$$-\frac{\partial \tilde{T}}{\partial \tilde{n}} = \frac{hL}{k} \tilde{T} \quad (9)$$

This equation reveals that the relative influence of the boundary condition depends on the ratio between the external ( $h$ ) and the internal ( $k/L$ ) heat transfer coefficients.

Equation (9) leads to another definition of thermally thin and thick structures, now with respect to the boundary conditions. Thin:  $L \ll k/h$ , thick:  $L \gg k/h$ . Applying a ratio of 1/10 for the thresholds, the structure is thin if  $L < 0.1 * k/h$ , and thick if  $L > 10 * k/h$ . The boundary conditions for the thin and thick approximations are:

$$\text{Thin: } \frac{\partial \tilde{T}}{\partial \tilde{n}} = 0, \text{ or } q = -k \frac{\partial T}{\partial n} = 0 \quad (10)$$

$$\text{Thick: } \tilde{T} = 0, \text{ or } T = T_a \quad (11)$$

For the case of a thin structure, the heat flux in the x-direction will totally dominate in equation (4), implying the approximation:

$$\frac{\partial^2 \tilde{T}}{\partial \tilde{x}^2} = 0 \text{ with } \frac{\partial \tilde{T}}{\partial \tilde{x}} = 0 \text{ on the two boundaries,} \quad (12)$$

implying that  $T$  does not vary in the x-direction. Then a simplified heat balance equation can be derived by integrating equation (1) in the x-direction, applying the boundary condition (2), and dividing by  $L$ :

$$\rho c_p \frac{\partial T}{\partial t} = 2 \frac{h(T_a - T)}{L} + \frac{\partial}{\partial y} \left( k \frac{\partial T}{\partial y} \right) + \frac{\partial}{\partial z} \left( k \frac{\partial T}{\partial z} \right) + Q \quad (13)$$

The same boundary condition has been assumed on both sides of the structure. Whether the terms for the y- and z-variation should be kept depends on the strength of their respective boundary conditions compared to the boundary conditions for heat flow in the x-direction. A detailed analysis is out of the scope for this paper, but if the heat transfer coefficients are the same on all sides, the terms can be neglected, and the equation is simplified to:

$$\rho c_p \frac{dT}{dt} = 2 \frac{h(T - T_a)}{L} + Q \quad (14)$$

This is a linear ordinary differential equation with time constant and characteristic heat density:

$$\tau = \frac{L \rho c_p}{2 h}, \quad Q_0 = \frac{2}{L} h(T_m - T_0) \quad (15)$$

We observe that the dependence on the thickness  $L$  has shifted from quadratic to linear, c.f. equations (7) and (8).

The approximated boundary condition, (10), was applied to show that  $T$  does not vary (significantly) in the x-direction, normal to the boundary. It must not be applied further, unless this is supported by additional analysis. The interpretation of thermally thin with respect to the boundary condition is that the ability to exchange heat with the surroundings is small compared to the ability to equilibrate the temperature within the structure in the normal direction. The capacity for heat transfer across the boundary can, however, be comparable to other terms and can therefore not be neglected in equation (13).

For the case of a thin structure in the x-direction, but thick with respect to the boundary conditions, we can apply equation (6), with boundary condition given by equation (11). For the stationary case the solution is:

$$T = T_a + \frac{Q}{2k} x(L - x) \quad (16)$$

In this analysis we have applied the total width,  $L$ , to define the non-dimensional variable,  $\tilde{x}$ , and similarly for  $W$  and  $H$ . The problem discussed, is, however, symmetric. Then all the variation takes place within half of the structure, and using the half-width is therefore more appropriate.

The general approach shown is a powerful tool to analyze a process and get insight about possible changes after a scale-up or scale-down. Equation (4) shows for instance that the aspect ratios are extremely important and that the thermal behavior qualitatively depends on the square of the aspect ratios. It is also clear that the time to reach equilibrium, or stationary conditions, increases with the square of the thickness, but boundary conditions must also be taken into account. For a thermally thin structure (with respect to boundary conditions), the time to reach the stationary state in-

creases *linearly*. The analysis reveals criteria to check how such behavior will be modified due to a change in scale. Finally, the analysis shows the relative strength of the various terms in the equations, and which terms may be disregarded in a first approximation. Studying the simplified equation can give valuable insight, even in cases where the approximation is not fully justified. In some cases a simple solution can be found, c.f. equation (16).

Some qualitative changes due to scale are well known. Consider for instance boiling a volume of water on the kitchen stove, and apply a length  $L$  to define the scale. The container area will be proportional to  $L^2$  and the water volume to  $L^3$ . If all linear dimensions are increased by a factor  $\beta$ , the heating area, and hence the heat supply, will be increased by the factor  $\beta^2$ ; while the water volume will be increased by  $\beta^3$ . Hence, the time needed to heat the water to the boiling point will be increased by the factor  $\beta^3/\beta^2 = \beta$ , assuming other factors to be negligible. This is an example of the  $L^{n+1}/L^{n+2}$  effect [1]. Such effects will be included in a proper mathematical analysis. In addition, it will be revealed whether such an effect will dominate, or whether other issues might be equally or more important.

## 2.2 Electrical Scale-up

General electrical scale-up has been studied for alternating current (AC) [2]. Some main results are presented below.

Assuming constant parameters and harmonic time variation, the equation for the electric field can be written as [2]:

$$\nabla^2 \vec{E} = i\omega\sigma_e\mu \vec{E} - \frac{\omega^2}{c^2} \vec{E} \quad (17)$$

where  $\vec{E}$  is the electric field vector;  
 $i$  is the imaginary unit;  
 $\omega$  is the angular frequency;  
 $\sigma_e$  is the electrical conductivity;  
 $\mu$  is the magnetic permeability;  
 $c$  is the speed of light;

A similar equation can be derived for the magnetic field.

If equation (17) is applied on a cuboid as shown in Figure 1, the same aspect ratios as found in equation (4), will show up in the non-dimensional version of the equation due to the Laplacian operator ( $\nabla^2$ ) on the left hand side. If relevant, this characteristic should be further analyzed. Here, we consider only the case where all geometric variables ( $x, y, z$ ) are non-dimensionalized by the same factor,  $L$ .

For simplification, we consider an electro-magnetic radiation propagating in the x-direction into an infinite half-plane of conducting media. In this case a linearly polarized electric field has only one non-zero component,  $E = E_z(x)$ , and the non-dimensional version of the equation can be written as [2]:

$$\frac{\partial^2 \tilde{E}}{\partial x^2} - 2i\left(\frac{L}{\delta}\right)^2 \tilde{E} + \left(2\pi\frac{L}{\lambda}\right)^2 \tilde{E} = 0 \quad (18)$$

where  $\delta$  is the skin depth;

$\lambda$  is the electromagnetic wave length;

$$\delta = \sqrt{\frac{2}{\omega\sigma_e\mu}}, \quad \lambda = \frac{2\pi c}{\omega} \quad (19)$$

Equation (18) shows that, in addition to the aspect ratio, there are two more non-dimensional parameters for the electric equation. Further, depending on the scale parameter,  $L$ , different regimes for the electric field can be defined:

- $L \gg \lambda$ , the last term must be included. Electromagnetic waves are important.
- $L \ll \lambda$  and  $\delta$  is not large compared to  $L$ . Alternating current (AC)
  - High frequency,  $\delta \ll L$ ,
  - Low frequency,  $\delta \sim L$  (same order of magnitude)
- $L \ll \lambda$  and  $L \ll \delta$ , the first term dominates and direct current (DC) approximation is valid

For our applications,  $L \ll \lambda$ , and electromagnetic waves can safely be neglected. Also, observe that the dependency on  $L/\delta$  is quadratic. Hence,  $(L/\delta)^2$  is the appropriate scale-up parameter to be considered. Further, the DC approximation is reasonable if  $L < \delta/5$  since the numerical factor in equation (18) then is less than 0.1.

It follows naturally that the concept of high and low frequency should not be defined by the frequency alone, but how the current behaves. Then  $(L/\delta)^2$  is the appropriate parameter where both size,  $L$ , material properties and frequency are included. For high frequencies, the electric current only flows very close to the surface of a conductor, while it penetrates significantly into the conductor in the low frequency domain.

If the largest width involved is applied as the scaling parameter,  $L$ , one can safely apply the DC approximation according to the criterion above, but this is frequently too conservative. For a single conductor in an insulating media the width of the conductor (or radius or diameter) is normally far more appropriate. For such cases, the thin approximation will normally be valid for the conductor and a simplified equation for the current distribution in the conductor can be derived.

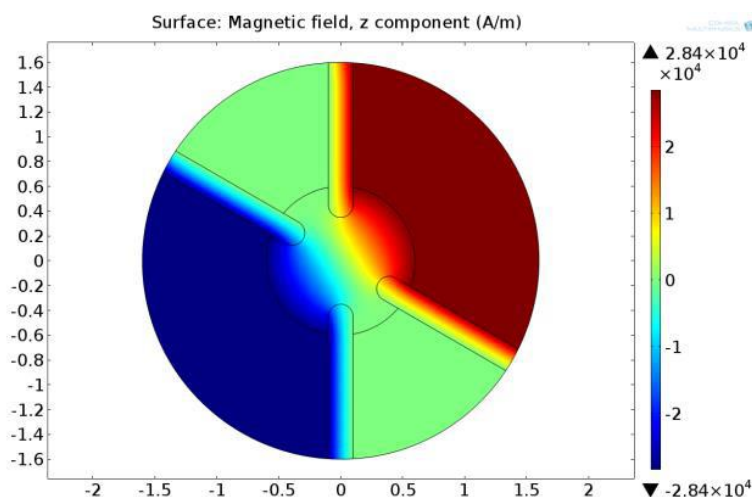


**Figure 2:** Magnetic field distribution for a 2D model in COMSOL Multiphysics. The alternating current flows into the central reactor via the two lower electrodes, and leaves via the two upper ones (and vice versa).

The conditions are more complex when more than one conductor is involved. For a 2D case (an approximation for currents flowing in sheets), it seems that  $L$  should be chosen as the sum of the widths of the sheets carrying the current. Figure 2 shows a case where the current is supplied to some reactor via two electrode pairs. The penetration of the magnetic field (and the electric current) into the electrodes is as if each electrode pair is replaced by one electrode with twice the thickness. The distribution is not influenced by the angle between the electrodes [2].

So far, we have not investigated the conditions for circular electrodes. It is well known that there is a proximity effect causing non-symmetric current distribution for the normal 3-phase 3 electrode configuration, c.f. for instance [3]. It is an open problem how to choose  $L$  for this system.

### 3 CASE STUDIES

#### 3.1 Resistive slag reactor

Consider a furnace where the required energy is supplied by resistive heating in a slag. Then scale up by increasing the slag zone by the same factor,  $\beta$ , in all directions. To keep the same reaction rate ( $\text{kg}/\text{m}^3 \text{ s}$ ) after scale-up, it is required to keep the power density, i.e.  $j^2 / \sigma_e$  should not change, where  $j$  is the current density (RMS-value for AC). The cross sectional area for the current will increase by the factor  $\beta^2$  due to the scale-up. Hence, the total current should increase by  $\beta^2$ .

This argument assumes that most of the power is utilized for chemical reactions. If the heat loss is significant, its influence will be relatively smaller after scale-up, c.f. the  $L^{n+1}/L^{n+2}$  effect [1]. Then the current should be increased somewhat less than by the factor  $\beta^2$  to ensure similar temperature conditions.

The argument is valid for DC, and for AC when the DC-approximation is reasonable. When the scale is adjusted by the same factor in all directions, there is no change in the aspect ratios. Further, there is no change in the local heat surplus when the same reaction rate and power density are assumed. The time constant to reach thermal equilibrium will, however, be increased by a factor  $\beta^2$ , c.f. equation (7).

If DC is not a proper approximation, the current distribution will be modified after scale-up.

In our analysis of electrical scale-up we have stated that the DC approximation is reasonable if  $L < \delta/5$ , c.f. paragraph 2.2. We believe that this is a rather strong requirement, i.e. it is likely that the current distribution is not *significantly* changed if the skin depth (after scale-up) is somewhat larger. Nevertheless, further analysis, simulations and/or experiments are recommended before concluding.

If AC-effects are significant, small-scale experiments with higher frequency might be valuable. Experiments with the same scaling parameter,  $(L/\delta)^2$ , will ensure the same current distribution.

Our analysis includes basic thermal and electrical scale-up, but material transport (solid, liquid, and/or gas flow) has not been considered. These effects should also be analyzed.

3.2 DC electrodes

For large electrodes, the risk of hard breakage limits the maximum electric current. This has been studied for many years by Elkem Carbon, c.f. for instance Larsen et al. [4].

We analyzed the thermal problem for large DC electrodes in the 97<sup>th</sup> European Study Group with Industry, Santiago the Compostela, Spain [5]. It was assumed that the aspect ratio,  $R/L$ , (radius divided by length) was less than 1/3, and that the thick structure boundary condition, equation (11), could be applied. We further assumed that the maximum temperature difference would be a measure of the risk of hard breakage. Hence, the scale-up criterion is that the maximum temperature is the same before and after scale-up.

A simplified equation similar to equation (6) can be derived for the axially symmetric problem. This equation has a simple solution and the maximum temperature in the center of the electrode can be written as [5]:

$$T_{max} = T_a + \frac{I^2}{\pi^2 R^2 k \sigma_e} \tag{20}$$

where  $I$  is the electrode current;

It follows that the electrode current should be increased proportionally to the radius (or diameter).

For very thin electrodes, we can apply the thin structure approximation, equation (10), which implies constant temperature across the electrode. It can then be shown that keeping this temperature requires that the electrode current is proportional to  $D^{3/2}$ , where  $D$  is the electrode diameter.

Westly has studied electrode consumption and correlated this to an electrode load factor. He then came up with the relation [6]:

$$I = C_E \frac{D^{3/2}}{\sqrt{\frac{R_{AC}}{R_{DC}}}} \tag{21}$$

where  $C_E$  is an electrode load factor and  $\sqrt{\frac{R_{AC}}{R_{DC}}}$  is a skin and proximity effect factor.

The skin and proximity factor is unity for small/thin electrodes and proportional to  $D^{1/2}$  for large electrodes, c.f. Figure 3.

The same  $C_E$  corresponds to similar electrode conditions. Hence, Westly's scale-up recommendation is the same as we find with very simple models: Electrode current proportional to  $D^{3/2}$  for small electrodes and proportional to  $D$  for large electrodes. Elkem Carbon recommends scale-up for medium and large electrodes as Westly, but proportional to  $D^2$  for small electrodes ( $D < 1$  m) [4],[7].

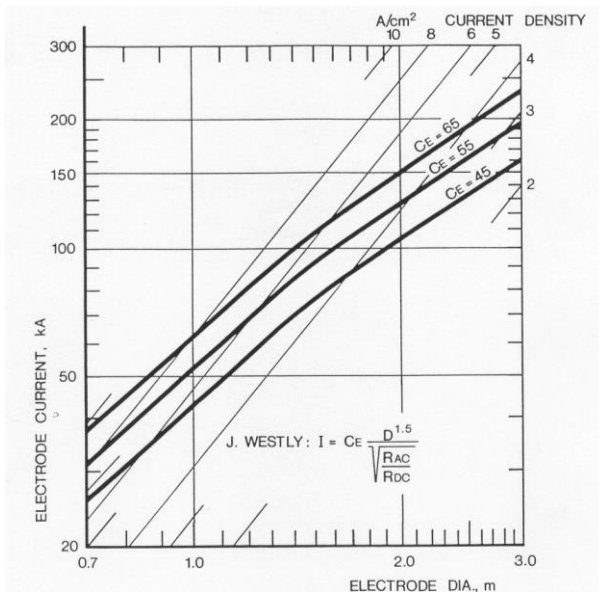


Figure 3: Electrode current versus diameter, according to Jens Westly. Figure courtesy of Elkem Carbon

As a simple estimate for the boundary conditions along a FeSi Søderberg electrode in the critical region, we will assume 1000 °C for both the boundary and the ambient temperatures, radiation condition and effective emissivity of 0.7. This corresponds to an effective heat transfer coefficient of 328 W/m<sup>2</sup> K, according to equation (3). We assume a heat conductivity of 8 W/m K, c.f. for instance Halvorsen et al. [8]. The thick electrode approximation is then very good for diameters above 0.5 m. If we assume a somewhat lower effective heat transfer coefficient, say 100 W/m<sup>2</sup> K, the approximation is very good for electrode diameters above 1.6 m. We conclude that the thick electrode approximation seems valid for large Søderberg electrodes, but more accurate estimates are required to determine the criterion for a large-diameter electrode.

Our criterion for thin electrodes,  $R < 0.1*k/h$ , is only valid for extremely thin electrodes, and does not seem relevant for

realistic sizes of Söderberg electrodes.

Our criteria for thin or thick electrodes, respectively  $R < 0.1*k/h$  and if  $R > 10*k/h$ , are rather strong. These criteria ensure that the respective approximations are quite good. The general scale-up trends are probably valid when one of the effects dominates, possibly if  $R < (1/3)*k/h$  or  $R > 3*k/h$ , with a gradual transition in-between. Numerical simulations are recommended to get further insight.

### 3.3 Thin Casting of Silicon

Elkem Technology has equipment for pilot testing of thin casting, c.f. Figure 4. Liquid metal is poured on a water spray cooled steel belt. The belt moves at a constant speed. A vital part of the pilot testing is to determine the proper length and/or speed of an industrial strip caster, and how these parameters depend on the height of the metal.

The overall solidification problem for casting of silicon was treated in a European Study Group with Industry (ESGI), which is a mathematical workshop.<sup>5</sup> The height of the casted metal will be small compared to the width and the length of the casted metal on the belt, with aspect ratios significantly lower than 1/3. Hence, it is only required to include heat conduction in the vertical direction for a mathematical analysis. There are two options for the mathematical problem:

- 2-dimensional model – Silicon enters the model at  $x = 0$  with a given temperature and height. There is a constant flow of silicon in the x-direction with the speed of the belt,  $v$ .
- Unidimensional dynamic model – At time  $t = 0$  the model assumes the given temperature and height of Si. Then the time evolution is computed based on the boundary conditions at the bottom and the top.
- The two formulations are equivalent. The time,  $t$ , in the unidimensional model corresponds to distance,  $x$ , according to the 2D model,  $x = vt$ .

The 2D formulation was chosen for the ESGI analysis. Constant parameters were assumed and the expansion of silicon during solidification was neglected. (The thermal effect of the latter can easily be included by appropriate modification of the thermal conductivity.) Further, constant temperature was assumed at the bottom, i.e. thick Si-layer with respect to the boundary condition.



**Figure 4:** Strip caster at Elkem Technology, principal sketch. Figure courtesy of Elkem Technology.

The analysis showed that a thin layer of frozen Si would evolve at the top, and a considerably thicker one from the bottom, c.f. Figure 5. The evolution of the upper layer is linear in time, while the lower has a quadratic dependence. The evolution of the lower one dominates, i.e. the model predicts quadratic dependence. Hence, if the metal height is doubled, the time required to freeze all the metal is increased by a factor four. Then the length of the belt must be increased by the same factor, if the speed is maintained.

Experiments showed, however, weak thermal contact between the steel belt and the silicon. This is partly due to a dust layer, which is difficult to avoid, and partly due to deformation of the silicon, which implies only partly contact with the steel/dust layer. If the thermal contact is sufficiently weak, the thin structure approximation is appropriate and linear behavior follows, i.e. the freezing time is proportional to the height. We postulate that the conditions are in-between linear and quadratic behavior.

<sup>5</sup> The first Mathematical Study Group with Industry was held in Oxford in 1968, the brainchild of the mathematicians Alan Tayler and Leslie Fox, who realised the importance and value of getting mathematicians together with industrialists. The study groups are now part of a European cooperation, and the concept has been exported worldwide, c.f. [9], [10], [11].

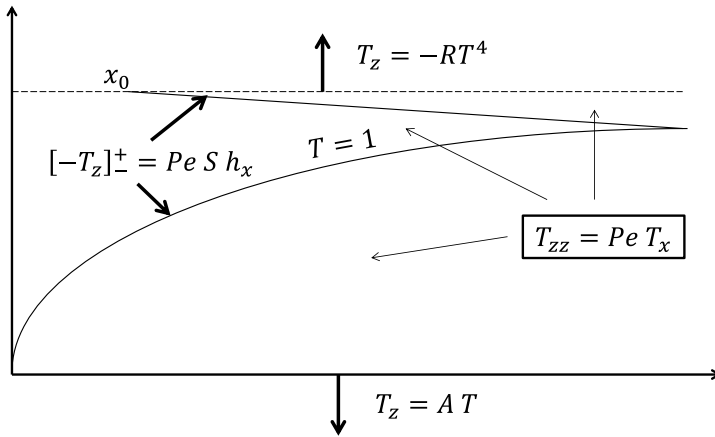


**Figure 5:** Dimensionless solidification problem from the ESGI analysis. Here, the “thin direction” is vertical, in the z-direction, and the x-direction is along the belt.

A numerical model was adapted in COMSOL Multiphysics to get further insight. In this model, we introduced an insulating layer between the steel belt and the silicon, where the strength of the thermal insulation easily can be changed and adapted to experimental measurements. The model revealed guidelines for experiments to determine the required time to freeze all liquid Si.

### 3.4 Acheson Furnace

Silicon Carbide is produced in large, open Acheson furnaces, c.f. Figure 6. These furnaces are rebuilt for each run. The raw materials are comparatively pure carbon and quartz particles, e.g. petroleum coke and quartz sand. Saw dust may be added to increase the porosity. The charge mix can be regarded as electrically non-conductive. Graphite rods and a core of coke particles are placed in the center of the furnace to ensure sufficient electric conduction at start-up [12].

After the preparations, high electric current is heating the materials for some 1-3 days, depending on the size of the furnace. The current is then turned off and the furnace is cooled. Unreacted raw materials are removed. The center of the furnace now consists of the following layers (from outside towards center): [12]

- Crust consisting of unreacted raw materials and SiO-condensate (SiO<sub>2</sub> and Si)
- Metallurgical grade SiC (β-SiC)
- Crystalline grade SiC (α-SiC)
- Graphite
- Void (possibly containing more or less of the original graphite rods and coke from the core)

We have developed and analyzed models for basic scale-up, i.e. considered how different scales of the process should be compared. The problem has been treated in an ESGI.

The chemical reactions for SiC-production are complex and many details are not known [12]. For thermal scale-up, it is possible to consider a simplified axially symmetric model. The main energy requirement is due to the production of β-SiC around 1600 °C according to the overall reaction:



Then β-SiC is converted to α-SiC at higher temperatures through gas-phase reactions [12]. These reactions require a small amount of energy compared to reaction (i). As a first approximation, we have neglected the thermal effect of the conversion from metallurgical to crystalline grade SiC. We have also neglected the crust formation and assumed that reaction (i) runs infinitely fast, i.e. the reaction takes place at a reaction front. Inside the front, there is SiC, and unreacted charge on the outside. At temperatures around 2700 °C SiC evaporates and a cavity is formed. The composition of the evaporated species has a molar ratio C/Si < 1, resulting in a surplus of C, which is left behind as a porous graphite structure [12]. We assume that the electrical conductivity of this “loose structure” is comparatively low.

Our analysis shows that the start-up of the furnace is special. From the start, only the core conducts the electrical current. Then, after some time, gradually more current can run in an SiC-layer, while the conductivity of the central core is reduced due to its removal.

By analysing the non-dimensional version of the equations, we have derived basic scale-up rules showing, among others, how the power should be changed when the diameter is increased. The analysis is valid as a first approximation. A numerical model is needed for more detailed results.

Gupta et al. [13] have previously developed an axially symmetric numerical simulation model. The model applies the following approximations:

- Only the overall reaction for SiC-production is included, reaction (i)
- Only standard heat conduction is modelled
  - Reaction (i) is included by an appropriate heat sink
- Heating by the electric current occurs only in a central resistor core

Today, improved simulation tools are available, e.g. COMSOL Multiphysics, and we recommend somewhat more details for suitable simulations. Including only the overall reaction is sufficient as a first approximation, but then the effect of more complex and realistic mechanisms should be studied. Transport of SiO-gas and SiO-condensation can be significant aspects of the heat balance [14], in addition to convection (mainly by CO flowing outwards). Heating by electrical current in the SiC-layer should also be included, along with reduced influence of the graphite core due to (at least some) disintegration.

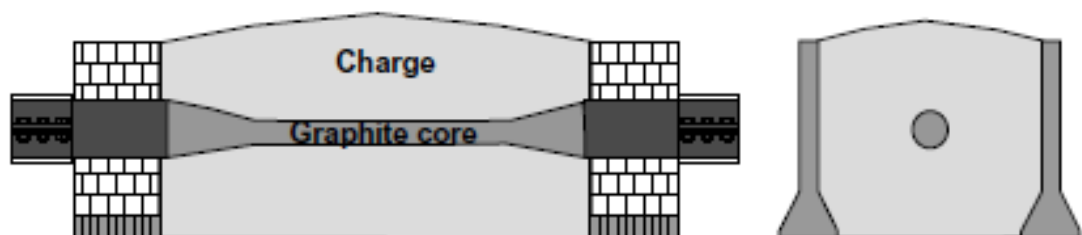


**Figure 5:** Principal sketch of an Acheson SiC furnace before a run. Figure from [12]

### 3.5 Metal Droplets in Slag

A problem related to metal-slag separation has been studied for Eramet. When a FeMn furnace is tapped, the metal and slag flow into a large ladle which then overflows into two subsequent ladles. The heavy molten metal should separate from the more viscous slag in the first ladle (metal ladle). From time to time, numerous metal droplets can be found in the slag in the second ladle. Previous studies by Eramet indicate that only sub millimeter metal droplets could represent a problem concerning settling time, but recent observations of frozen slag ladles reveal as large as 0.5-1 cm metal droplets trapped in slag. The scale-up issue was to interpret some small-scale experiments and possibly propose further laboratory tests. Mathematical models should be applied to bridge the gap between experimental studies and industrial experience.

This problem has been treated in workshops at the University of Oxford and the University of Santiago de Compostela. So far, we have only performed a limited mathematical analysis:

- Initial evaluation of droplet settling (single droplets)
- Unidimensional model for many droplets in slag (many particles slow down the settling)
- Basic mechanisms when a jet falls into a stratified fluid

The initial analysis and discussions with Eramet clearly indicate that droplets form as slag and metal flow as a jet into the metal ladle, where the mixture is already stratified and partially separated. The droplet formation rate, the droplet coalescence rate and the general flow within the ladle all have a significant influence on the amount of metal droplets that overflows into the second ladle. We intend to follow up this initial study in a student project within the framework of Oxford University's EPSRC Centre for Doctoral Training (CDT) in Industrially Focused Mathematical Modelling.

## 4 DISCUSSION

As a general guideline, we recommend the following for evaluating scale-up/scale-down:

- Establish mathematical equations describing the relevant/critical processes
- Reformulate the equations in non-dimensional form
- Identify the non-dimensional parameters
- Determine how these parameters are affected by scale-up/scale-down
- Study/analyze the effect of modified parameters due to scale-up/scale-down
- Study limiting cases, when one or more parameters are large or small compared to others
- Perform some comparatively simple numerical studies as supplements to the analysis

Such studies will improve the understanding and reveal what needs to be further examined, by more detailed simulations and/or experiments.

It is vital that the models are properly interpreted. Thin with respect to boundary condition means, for instance, that the ability to equilibrate the temperature in the direction normal to the boundary is considerable compared to the ability to exchange heat with the surroundings; and vice versa for a thick construction – not necessarily corresponding to the everyday use of thin/thick.

Simplifications may result in adequate models. We recommend that the necessary assumptions are reviewed afterwards to check whether the results of the analyses/computations are reasonable.

The mathematical analysis is a powerful tool to reveal general trends. Consider electrical scale-up as an example

- For a general slag process, the total current should be approximately proportional to the square of the effective cross section for the current. Here, the dominating factor is to ensure the same current density to enable the same reaction speed.
- For an electrode the dominating aspect is to “get rid of” surplus heat. Then the current should be proportional to  $D^{3/2}$  or  $D$ , depending on whether the electrode is “thin” or “thick”; with some transition in-between.
- Consequently, the electrode diameter does not scale up similar to the process. The larger the active process region, the larger the relative diameter of the electrodes. Such an effect needs to be studied further.

## 5 CONCLUSIONS

We recommend that appropriate mathematical models and analyses are applied for evaluating metallurgical scale-up or scale-down. Such models are powerful tools to reveal general trends and what needs to be further studied; either by numerical simulations, laboratory experiments, and/or pilot studies.

Based on our experience we have derived a general guideline for such mathematical analyses.

## 6 REFERENCES

- [1] Tatterson, G. B., “Process Scaleup and Design”, Compendium, ISBN: 0-9726635-0-9, 2002.
- [2] Schlanbusch, R., Halvorsen, S.A., Shinkevich, S., Gómez, D., “Electrical Scale-Up of Metallurgical Processes”, COMSOL Conference, Cambridge, UK, 2014
- [3] Bermúdez, A., Gómez, D., Salgado, P., “Mathematical Model and Numerical Simulation in Electromagnetism”, UNITEXT – La Matematica per il 3+2, Springer 2014.
- [4] Larsen, B., Feldborg, H., Halvorsen, S.A., “Minimizing Thermal Stress During Shutdown of Søderberg Electrodes”, INFACON XIII, Almaty, Kazakhstan, 2013.
- [5] Bermúdez, A., Cregan, V., Gómez, D., Rial, Á., Vázquez, R., Halvorsen, S.A., “Electric scale-up for a slag heating furnace”, In: Proceedings of the 97th European Study Group with Industry (ESGI). Eds. Bermúdez, A., Man-teiga, W.G, Quintela y José Antonio Vilar. P., pp. 7-31, Santiago de Compostela, Spain, 2015.
- [6] Westly, J., “Electrode consumption in Production of 75 % FeSi and Si-met”, Electric Furnace Conference, Toronto 1984.
- [7] Innvær, R., “A Status for the Søderberg Smelting Electrode”, ELECTROTECH’92, Montreal 1992.
- [8] Halvorsen, S.A., Valderhaug, Aa.M., Fors, J., “Basic Properties of the Persson Type Composite Electrode”, Electric Furnace Conference, Pittsburgh, 1999.
- [9] <http://www.esgi.org.uk/>, the official website for the European Study Groups with Industry in UK
- [10] [http://www.ecmi-indmath.org/?page\\_id=104](http://www.ecmi-indmath.org/?page_id=104), information of recent and upcoming European Study Groups with Industry (ESGIs)
- [11] <http://miis.maths.ox.ac.uk/how/>, information on Study Groups with Industry
- [12] Lindstad, L.H., “Recrystallization of Silicon Carbide”, Dr. ing. thesis, Department of Materials Technology and Electrochemistry, NTNU, Trondheim, Norway, 2002
- [13] Gupta, G.S., Kumar, P.V., Rudolph, V.R., Gupta, M., “Heat-Transfer Model for the Acheson Process”, Metallurgical and Materials Transactions A, Vol. 32A, June 2001
- [14] Schei, A., Tuset, J.K., Tveit, H., “Production of high silicon alloys”, Tapir, Trondheim, Norway, 1998

## 7 ACKNOWLEDGEMENT

The authors would like to thank Regional Research Fund Agder (RFF Agder) for their financial support.